

PACS numbers: 81.07.Bc; 42.70.Hj; 42.55.Rz; 78.60.Lc
DOI: 10.1070/QE2012v042n09ABEH014919

Structural, spectral-luminescent, and lasing properties of nanostructured $Tm:CaF_2$ ceramics

P.A. Ryabochkina, A.A. Lyapin, V.V. Osiko, P.P. Fedorov, S.N. Ushakov, M.V. Kruglova, N.V. Sakharov, E.A. Garibin, P.E. Gusev, M.A. Krutov

Abstract. **The structure and the spectral-luminescent properties of CaF_2-TmF_3 fluoride ceramics and single crystals are studied. AFM investigations revealed a layered nanostructure of grains, which was not observed in reference samples of single crystals. It is found that the spectral-luminescent properties of CaF_2-TmF_3 ceramics and single crystals are similar. Lasing at the $^3F_4 \rightarrow {}^3H_6$ transition of Tm^{3+} ions in CaF_2-TmF_3 ceramics (wavelength 1898 nm) under diode pimping is obtained for the first time.**

Keywords: *fluoride laser ceramics, nanostructure, two-micron lasing.*

1. Introduction

The technology of oxide laser ceramics is an important achievement of recent years in the fields of optical material science and laser physics [1–3]. Output power of 100 kW was achieved in solid-state lasers with active elements of yttrium aluminum garnet ceramics doped with Nd^{3+} ions [4].

Of great practical interest are works on the creation of a technology of fluoride laser ceramics, which has better mechanical properties than single crystals and retains their spectral-luminescent properties [5–8]. Lasing has already been obtained in fluoride ceramics with F^{2-} colour centres [9], as well as in fluoride ceramics doped with Dy^{2+} [5], Yb^{3+} [8, 10, 11], Nd^{3+} [12], and Pr^{3+} [13] ions.

At present, extensive investigations are carried out on the creation of solid-state lasers based on Tm^{3+}-doped materials emitting in the two-micron wavelength region. This radiation is used in medicine and lidars, as well as for frequency conversion to the mid-IR region. Review [14] presents data on two-micron lasing obtained in different crystals, for example, $Tm:Y_3AlO_{12}$, $Tm:Lu_2O_3$, and $Tm:Sc_2O_3$. The structural, spectral-luminescent, and lasing properties of $Tm:Lu_2O_3$ ceramics were studied in [15].

In addition to Tm^{3+}-doped oxide crystals and ceramics, of interest are Tm^{3+}-doped fluoride materials. In the CaF_2-TmF_3 system, $Ca_{1-x}Tm_xF_{2+x}$ solid solutions are formed within a wide homogeneity range ($x \geqslant 0.40$) [16]. The solid solution phase diagram allows one to grow single crystals of high optical quality with TmF_3 concentrations up to 15 mol% [17, 18]. The thermal conductivity of $Ca_{1-x}Tm_xF_{2+x}$ single crystals was measured in [19]. Lasing in $Tm^{3+}:CaF_2$ single crystals pumped by a $Ti:Al_2O_3$ laser was obtained in [20].

The results of our investigations of the structure and the spectral-luminescent properties of $Tm:CaF_2$ ceramics produced by hot pressing were reported in [21].

In this paper, we present the results of the first experiment on two-micron lasing in diode-pumped $Tm:CaF_2$ ceramics ($^3F_4 \rightarrow {}^3H_6$ transition), as well as the results of more detailed investigations of the structure and the spectral-luminescent properties of this ceramics in comparison with $Tm:CaF_2$ single crystals.

2. Characteristics of samples and experimental technique

The samples of CaF_2-TmF_3 single crystals and ceramics were produced in the INKROM Ltd and the A.M. Prokhorov General Physics Institute, Russian Academy of Sciences.

The CaF_2-TmF_3 solid-solution single crystals were grown by vertical directed crystallisation (Bridgman method) in platinum crucibles in a vacuum furnace with a graphite resistance heater and graphite heat shields. The samples of CaF_2-TmF_3 ceramics were produced by deep plastic deformation (hot pressing). Hot pressing was performed at a temperature of 1150 °C and a pressure of 0.6 tf cm^{-2}; the degree of deformation of the initial billet was 400%.

We studied the spectral-luminescent properties of samples of CaF_2-TmF_3 single-crystals and ceramics with dimensions of $1.5\times10\times12$ and $5\times14\times16$ mm, respectively.

The active elements made of CaF_2-TmF_3 ceramics for laser experiments had the form of a parallelepiped $3\times3\times5$ mm in size. The faces of the active elements were antireflection coated for the laser wavelength ($\lambda_{gen} \sim 2$ μm).

The structure of CaF_2-TmF_3 ceramics and single crystals was studied using a Jeol JSM-6490 (JEOL, Japan) scanning electron microscope. The surface morphology of samples was studied with a Solver Pro (NT-MDT, Zelenograd, Russia) atomic force microscope (AFM).

The absorption spectra of Tm^{3+} ions in the studied crystals and ceramics were recorded by a PerkinElmer Lambda 950 double-beam double-monochromator scanning spectrophotometer.

The luminescent properties of fluoride single crystals and ceramics doped with Tm^{3+} ions were studied using a computer-controlled setup based on an MDR-23 monochromator. The

P.A. Ryabochkina, A.A. Lyapin N.P. Ogarev Mordovian State University, ul. Bol'shevistskaya 68, 430005 Saransk, Russia; e-mail: ryabochkina@freemail.mrsu.ru;
V.V. Osiko, P.P. Fedorov, S.N. Ushakov A.M. Prokhorov General Physics Institute, Russian Academy of Sciences, ul. Vavilova 38, 119991 Moscow, Russia;
M.V. Kruglova, N.V. Sakharov N.I. Lobachevsky Nizhnii Novgorod State University, prosp. Gagarina 23, 603950 Nizhnii Novgorod, Russia
E.A. Garibin, P.E. Gusev, M.A. Krutov INKROM Ltd, ul. Babushkina 36, bld. 1, 193171 St. Petersburg, Russia

Received 13 June 2012; revision received 13 July 2012
Kvantovaya Elektronika **42** (9) 853–857 (2012)
Translated by M.N. Basieva

luminescence of Tm^{3+} ions from the $^3H_4$ level was excited by a laser diode radiation with $\lambda_p \sim 800$ nm. Luminescence spectra were recorded with synchronous detection of signals using an SR-810 lock-in amplifier. As radiation detectors in different spectral regions, we used a FEU-79 photomultiplier, an FD-7G photodiode, and a PbS photoresistor.

In laser experiments, the active elements cut of CaF_2–TmF_3 single crystals and ceramics were optically pumped by a fibre-coupled (fibre diameter 400 μm) laser diode array with the maximum output power of 60 W.

The lasing spectrum of CaF_2–TmF_3 ceramics was recorded by a computer-controlled system based on an MDR-23 monochromator with the use of an SR250 Boxcar integrator detection system.

3. Structure of CaF_2–TmF_3 single crystals and ceramics

Photographs of the surface structure of CaF_2–TmF_3 (4 mol%) ceramics with different magnifications obtained by scanning electron microscopy (SEM) are given in Fig. 1.

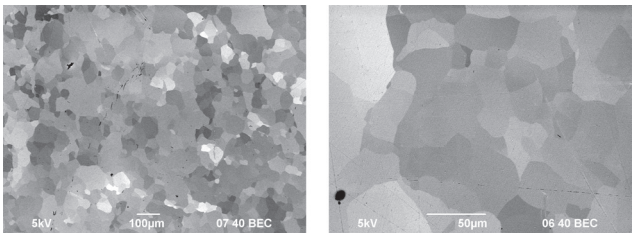

Figure 1. Microphotographs of the surface of CaF_2–TmF_3(4 mol%) ceramics.

The photographs show that the grain structure of ceramics is strongly inhomogeneous. Analysing the presented images, one can see that the crystallites are significantly different in size, namely, the smallest crystallites do not exceed 10 μm and the largest crystallites reaches 100 μm in size.

The SEM microphotographs of the cleavage surfaces of CaF_2–TmF_3(4 mol%) ceramics and single crystals (Fig. 2) show that the cleavages of single crystals have the form of triangular steps with inhomogeneities observed on the tops of some steps, while ceramics of the same composition demonstrates a layered structure.

The cleavages of CaF_2–TmF_3 (4 mol%) ceramics and single crystals were studied in detail by AFM. The measurements were performed in air in the contact regime using silicon I-shaped NT-MDT NSG-11 cantilevers with the corner radius $R < 10$ nm (rated value). The maximum resolution of AFM measurements was 10 nm in the surface plane and 1 nm in height.

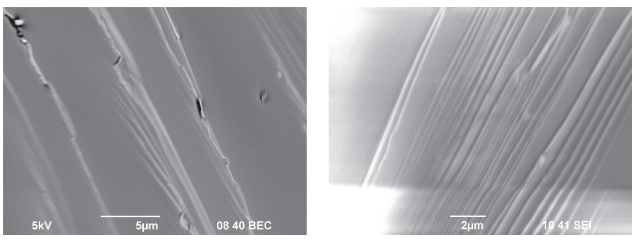

a b

Figure 2. Microphotographs of the cleavage surfaces of a CaF_2–TmF_3(4 mol%) single crystal (a) and ceramics (b).

Figure 3 shows an AFM image of the surface of CaF_2–TmF_3(4 mol%) ceramics. One can see that the grains are characterised by a layered structure with the layer thickness of 150–300 nm (Fig. 4). The layered structure of the grains of CaF_2–TmF_3 ceramics observed in our experiments is similar to the structure obtained previously by AFM in CaF_2 and $Nd:CaF_2$ ceramics [8].

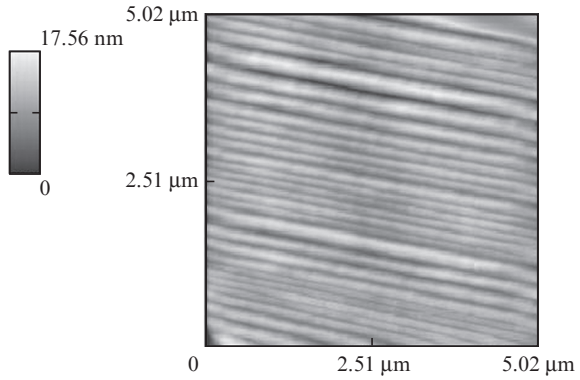

Figure 3. AFM image of the morphology of the fracture surface of CaF_2–TmF_3(4 mol%) ceramics.

The AFM images of the cleavage surface morphology of a CaF_2–TmF_3(4 mol%) single crystal are shown in Fig. 5. One sees that the cleavage surface is imperfect. At the same time, some images demonstrate the presence of atomically smooth regions on the single crystal cleavages with a thickness of 1600 nm. The profiles of cross sections cut perpendicular to the direction of layers (Fig. 6) allow us to determine the average layer height to be 10–70 nm.

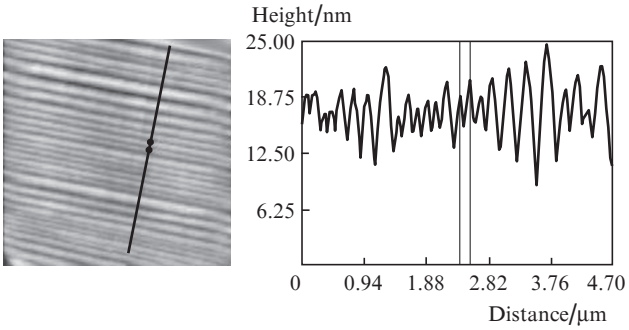

Figure 4. Profile of the cross section cut perpendicular to the layers of CaF_2–TmF_3(4 mol%) ceramics.

Analysing the AFM and SEM images of the cleavages of single crystals and the fractures of CaF_2–TmF_3 ceramics, we can see that the stratification typical for CaF_2–TmF_3 ceramics is absent in the reference samples of single crystals. The studied single crystals are characterised by less perfect cleavage than pure fluorite crystals [7].

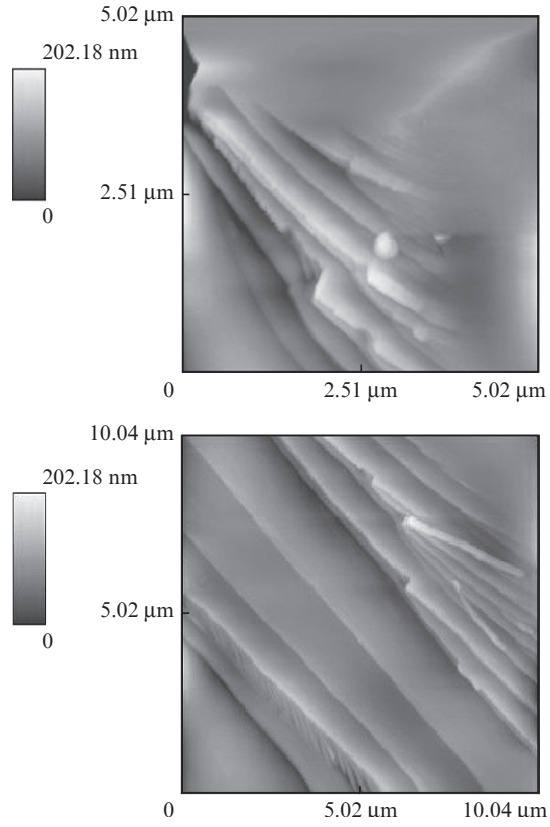

Figure 5. AFM images of the morphology of the cleavage surface of a CaF_2–TmF_3 (4 mol%) single crystal.

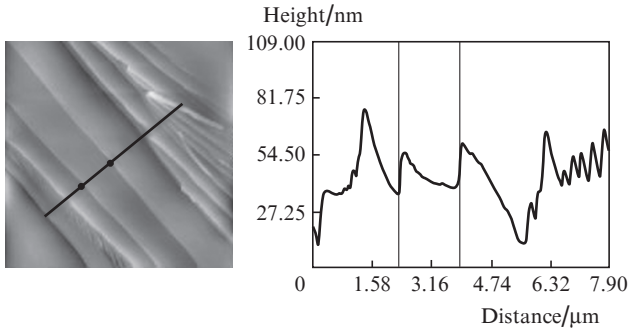

Figure 6. Profile of the cross section cut perpendicular to the layers of a CaF_2–TmF_3 (4 mol%) single crystal.

4. Spectral-luminescent properties of CaF_2–TmF_3 single crystals and ceramics

The absorption due to the transition of Tm^{3+} ions from the ground $^3H_6$ state to the excited $^3H_4$ state in thulium-doped crystals and ceramics plays an important role in two-micron lasing at the $^3F_4 \rightarrow {}^3H_6$ transition of Tm^{3+} ions. The $^3H_4$ level of Tm^{3+} ions is populated under laser diode pumping ($\lambda_p \sim$ 790 nm), and then the upper laser level $^3F_4$ is populated due to the cross relaxation $^3H_4 \rightarrow {}^3F_4$, $^3H_6 \rightarrow {}^3F_4$. The absorption spectrum of CaF_2–TmF_3 (4 mol%) ceramics and single crystals corresponding to the $^3H_6 \rightarrow {}^3H_4$ transition of Tm^{3+} ions is shown in Fig. 7. As is seen, the absorption spectra of single crystals and ceramics are very similar. The slight difference in the peak values of the absorption of ceramics and single crystals is explained, in our opinion, by some difference in the concentrations of dopants in the studied samples of single crystals and ceramics.

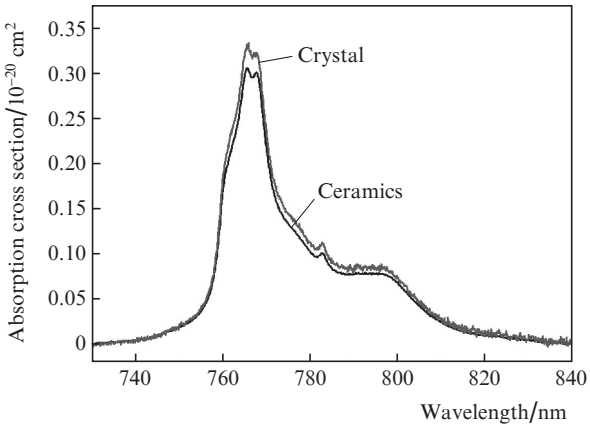

Figure 7. Absorption spectra of CaF_2–TmF_3 (4 mol%) ceramics and single crystals at $T = 300$ K ($^3H_6 \rightarrow {}^3H_4$ transition).

In order to obtain two-micron lasing at the $^3F_4 \rightarrow {}^3H_6$ transition of Tm^{3+} ions, it was interesting to study the luminescence spectrum of this transition and to estimate the spectral dependence of the gain cross section of the laser transition using the spectral dependences of luminescence and absorption cross sections for the $^3F_4 \rightarrow {}^3H_6$ transitions of Tm^{3+} ions. The knowledge of this dependence is important for choosing laser cavity mirrors for laser experiments.

The spectral dependence of the luminescence cross section of the stimulated $^3F_4 \rightarrow {}^3H_6$ transition of Tm^{3+} ions at the temperature $T = 300$ K was determined by the Füchtbauer–Ladenburg formula [22]

$$\sigma_{em}(\lambda) = \frac{\lambda^5 I(\lambda)}{8\pi c \tau_{rad} n^2 \int I(\lambda)\lambda \, d\lambda}, \quad (1)$$

where λ is the wavelength, I is the relative luminescence intensity, n is the refractive index of the medium for the corresponding wavelength, τ_{rad} is the radiative lifetime of the excited level of the corresponding rare-earth ion transition, and c is the speed of light. We used the refractive index $n = 1.42$ and the radiative lifetime $\tau_{rad} = A^{-1} = 14.2$ ms. Here, A^{-1} is the probability of the radiative transition from the $^3F_4$ level, which was estimated by the formula [23]

$$A = \frac{8\pi n^2 c}{N_0 \lambda^4} \frac{2J' + 1}{2J + 1} \int k(\lambda) \, d\lambda, \quad (2)$$

where N_0 is the concentration of dopant atoms, $k(\lambda)$ is the absorption coefficient, J' and J are the total angular momenta of 4f electrons in the ground and excited states of the transition.

The spectral dependences of the absorption and luminescence cross sections for the $^3H_6 \leftrightarrow {}^3F_4$ transitions of Tm^{3+} ions at $T = 300$ K for CaF_2–TmF_3 (4 mol%) single crystals and ceramics are shown in Fig. 8. One can see that these dependences are identical.

Using the spectral dependences of the absorption and luminescence cross sections σ_{abs} and σ_{em} for the $^3H_6 \rightarrow {}^3F_4$ and $^3F_4 \rightarrow {}^3H_6$ transitions of Tm^{3+} ions, we found the wave-

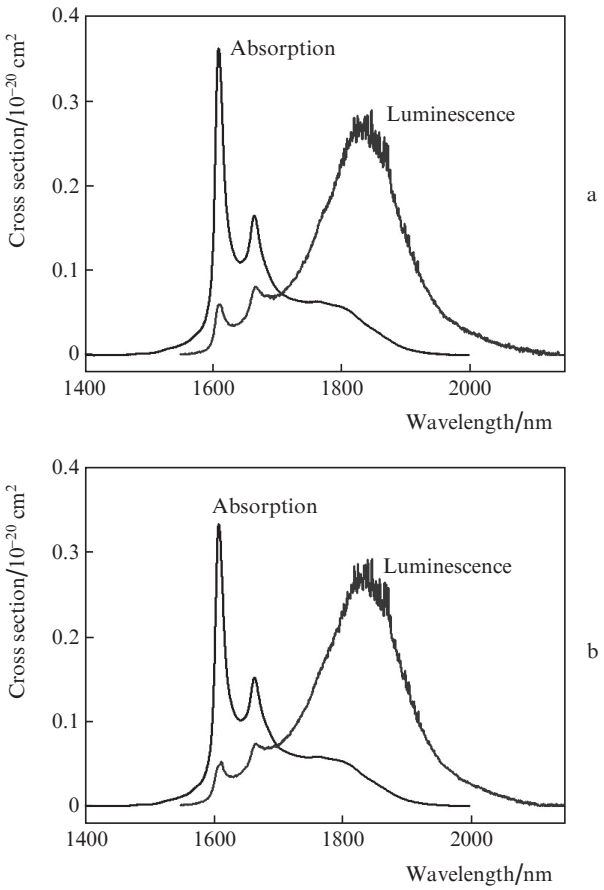

Figure 8. Absorption ($^3H_6 \rightarrow {}^3F_4$ transition of Tm^{3+} ions) and luminescence ($^3F_4 \rightarrow {}^3H_6$ transition) spectra of CaF_2–TmF_3(4 mol%) single crystals (a) and ceramics (b) at $T = 300$ K.

length dependence of the gain cross section σ_g of the expected laser transition $^3F_4 \rightarrow {}^3H_6$ in the form [24]

$$\sigma_g(\lambda) = P\sigma_{em}(\lambda) - (1 - P)\sigma_{abs}(\lambda), \quad (3)$$

where P is the relative population inversion of levels. Figure 9 shows the dependences $\sigma_g(\lambda)$ for the parameter P equal to 0.06, 0.07, 0.08, 0.09, and 0.1. As seen from the figure, the gain region of CaF_2–TmF_3 (4 mol%) ceramics extends from 1850 to 2000 nm.

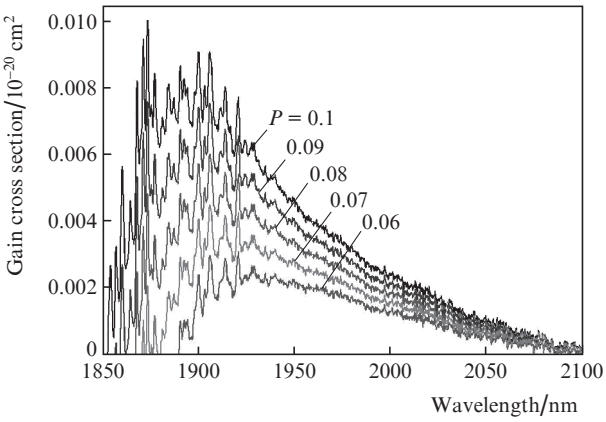

Figure 9. Spectral dependence of the gain cross section $\sigma_g(\lambda)$ ($^3F_4 \rightarrow {}^3H_6$ transition) of CaF_2–TmF_3(4 mol%) ceramics at different values of relative population inversion P at $T = 300$ K.

5. Lasing properties of Tm : CaF_2 ceramics

The optical scheme of a laser used to obtain and study lasing at the $^3F_4 \rightarrow {}^3H_6$ transition of Tm^{3+} ions in CaF_2–TmF_3 (4 mol%) ceramics is shown in Fig. 10. The active element was pumped to the $^3H_4$ level of Tm^{3+} ions by a laser diode array (*1*) with a fibre pigtail (*2*) (wavelength 798 nm). To reduce the thermal load on the active element, we used a chopper (*4*), which formed pump pulses with a duration of 20 ms and a repetition rate of ~2 Hz. The pump radiation was projected into the sample in a 1:1 proportion by an objective (*3*). The temperature of the active element holder was kept at ~18 °C by a temperature stabilisation system.

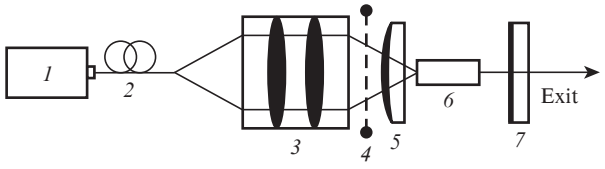

Figure 10. Optical scheme of a laser based on CaF_2–TmF_3(4 mol%) ceramics:
(*1*) laser diode arrays; (*2*) optical fibre; (*3*) objective; (*4*) chopper; (*5*) input mirror; (*6*) active element; (*7*) output mirror.

The laser cavity was formed by an input spherical mirror (*5*) (with the working surface radius of curvature of 300 mm, the transmission coefficient at the pump wavelength no less than 90%, and the reflection coefficient at the laser wavelength higher than 99%) and a plane output mirror (*7*) with a transmission coefficient at the laser wavelength below 1%. The cavity length was 15 mm.

The dependence of the average output power of the laser based on CaF_2–TmF_3 (4 mol%) ceramics on the average pump power is given in Fig. 11. Under the conditions of the described laser experiment, the laser slope efficiency was 5.5%.

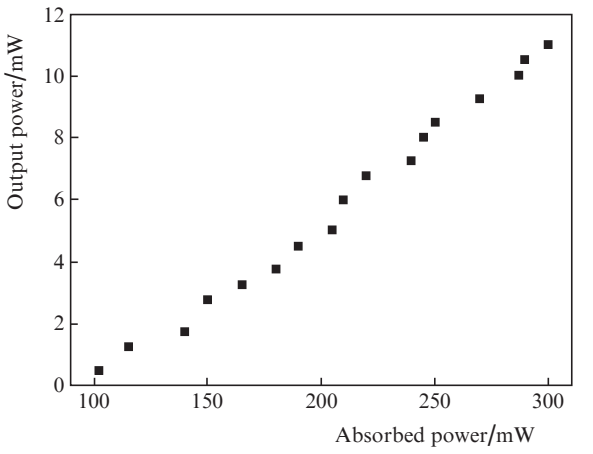

Figure 11. Dependence of the average laser output power on the average absorbed pump power for CaF_2–TmF_3(4 mol%) ceramics.

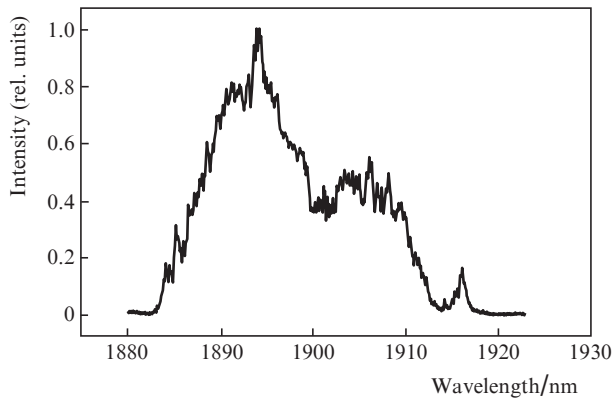

Figure 12. Lasing spectrum of CaF_2-TmF_3 (4 mol%) ceramics.

The lasing spectrum of CaF_2-TmF_3 (4 mol%) ceramics is presented in Fig. 12.

6. Conclusions

The structural, spectral-luminescent, and lasing properties of Tm^{3+}-doped CaF_2 single crystals and ceramics are studied in order to use these materials as active media of solid-state two-micron lasers.

We obtained the following results.

(i) Investigations of CaF_2-TmF_3 (4 mol%) ceramics revealed that its grain structure is hierarchical. The size of the finest grains does not exceed 10 μm, and the largest grains reach a size of 100 μm.

(ii) The AFM investigations showed that the grains have a layered nanostructure comprising a system of lamellas with a characteristic thickness of 150–300 nm.

(iii) The spectral dependence of the luminescence cross section for the $^3F_4 \rightarrow {}^3H_6$ transition of Tm^{3+} ions is studied for the ceramics and single crystal. The gain region of both materials for the relative population inversion P varying from 0.06 to 0.1 corresponds to the spectral range of 1850–2000 nm.

(iv) Lasing at a wavelength of 1898 nm was obtained on the $^3F_4 \rightarrow {}^3H_6$ transition of Tm^{3+} ions in the CaF_2-TmF_3 (4 mol%) ceramics under diode laser pumping. The lasing slope efficiency was 5.5%.

Acknowledgements. This work was supported by the Federal Targeted Program 'Scientists and Science Educators of Innovative Russia' for 2009–2013 years (State Contract No. 14.740.11.0071).

References

1. Ikesue A., Kinoshita T., Kmata K., Yoshida K. *J. Am. Ceram. Soc.*, **78**, 1033 (1995).
2. Lu J.R., Lu J.H., Murai T., Uematsu T., Shirakava A., Ueda K., Yagi H., Yanagitani T., Kaminskii A.A. *Japan. J. Appl. Phys. Part 2 (Lett.)*, **40** (12A), L1277 (2001).
3. Takaichi K., Lu J.R., Murai T., Uematsu T., Shirakawa A., Ueda K., Yagy H., Yanagitani T., Kaminski A.A. *Japan. J. Appl. Phys. Part 2 (Lett.*), **41** (2A), L96 (2002).
4. Sanghera J., Shaw B., Kim W., Villalobos G., Baker C., Frantz J., Hunt M., Sadowski B., Aggarwal I. *Proc. SPIE Int. Soc. Opt. Eng.*, **7912**, 79121Q-1 (2011).
5. Hatch S.E., Parsons W.F., Weagley R.J. *Appl. Phys. Lett.*, **5** (8), 153 (1964).
6. Fedorov P.P., Osiko V.V., Basiev T.T., Orlovskii Yu.V., Dukel'skii K.V., Mironov I.A., Demidenko V.A., Smirnov A.N. *Ros. Nanotechnol.*, **2** (5-6), 95 (2007).
7. Akchurin M.Sh., Gainutdinov R.V., Garibin E.A., et al. *Perspectivnye Materialy*, (5), 5 (2010).
8. Fedorov P.P., Osiko V.V., Kuznetsov S.V., Garibin E.A. *Fluoride laser nanoceramics. 4th Intern. Forum Nanotechnology (RUSNANOTECH)* (Moscow, 2011); *J. Phys. Conf. Ser.*, **345**, 012017 (2012). DOI:10.1088/1742-6596/345/1/012017.
9. Basiev T.T., Doroshenko M.E., Konyushkin V.A., Osiko V.V., Ivanov L.I., Simakov S.V. *Kvantovaya Elektron.*, **37** (11), 989 (2007) [*Quantum Electron.*, **37** (11), 989 (2007)].
10. Basiev T.T., Doroshenko M.E., Fedorov P.P., Konyushkin V.A., Kuznetsov S.V., Osiko V.V., Akchurin M.Sh. *Opt. Lett.*, **33** (5), 521 (2008).
11. Alimov O.K., Basiev T.T., Doroshenko M.E., Fedorov P.P., Konyushkin V.A., Kouznetsov S.V., Nakladov A.N., Osiko V.V., Shlyakova O.V. *Proc. Intern. Conf. Lumin. Opt. Spectrosc. Condens. Matter (ICL)* (Lyon, France, 2008).
12. Basiev T.T., Doroshenko M.E., Konyushkin V.A., Osiko V.V. *Opt. Lett.*, **35**, 23 (2010).
13. Basiev T.T., Konyushkin V.A., Konyushkin D.V., Doroshenko M.E., Huber G., Reishert F., Hansen N.O., Fechner M. *Opt. Mater. Express*, **1** (8), 1511 (2011).
14. Scholle K., Lamrini S., Koopmann P., Fuhrberg P. *Frontiers. Guided Wave Optics and Optoelectronics.* (Rijeka: InTech, 2010).
15. Antipov O.L., Golovkin S.Yu., Gorshkov O.N., et al. *Kvantovaya Elektron.*, **41** (10), 863 (2011) [*Quantum Electron.*, **41** (10), 863 (2011)].
16. Sobolev B.P., Fedorov P.P. *J. Less-Common Metals*, **60**, 33 (1978). DOI: 10.1016/0022-5088(78)90087-5.
17. Fedorov P.P., Osiko V.V. in *Bulk Crystal Growth of Electronic, Optical and Optoelectronic Materials*. Ed. by P.Capper (Chichester: John Wiley & Sons, Ltd., 2005) p. 339.
18. Kuznetsov S.V., Fedorov P.P. *Inorg. Mater.*, **44** (13), 1434 (2008). DOI: 10.1134/S0020168508130037.
19. Popov V.A., Fedorov P.P., Reiterov V.M., Garibin E.A., Demidenko A.A., Mironov I.A., Osiko V.V. *Dokl. Akad. Nauk*, **443** (3), 304 (2012).
20. Gamy P., Doualan J.L., Renard S., Braud A., Menard V., Moncorge R. *Opt. Commun.*, **236**, 4 (2004).
21. Bol'shchikov F.A., Garibin E.A., Gusev P.E., Demidenko A.A., Kruglova M.V., Krutov M.A., Lyapin A.A., Mironov I.A., Osiko V.V., Reiterov V.M., Ryabochkina P.A., Sakharov N.V., Smirnov A.N., Ushakov S.N., Fedorov P.P. *Kvantovaya Elektron.*, **41** (3), 193 (2011) [*Quantum Electron.*, **41** (3), 193 (2011)].
22. Weber M.J. (Ed.) *Handbook of Laser Science and Technology* (Boka Raton: CRC Press, 1982) Vol. 1.
23. Basiev T.T., Zharikov E.V., Zhekov V.I., Murina T.M., Osiko V.V., Prokhorov A.M., Starikov B.P., Timoshechkin M.I., Shcherbakov I.A. *Kvantovaya Elektron.*, **3** (7), 1471 (1976) [*Quantum Electron.*, **6** (7), 796 (1976)].
24. Petrov V., Guell F., Massons J., Gavalda J., Sole R.M., Aguilo M., Diaz F., Griebner U. *IEEE J. Quantum Electron.*, **40** (9), 1244 (2004).